

## CONSERVING TIME-INTEGRATION OF BEAMS UNDER CONTACT CONSTRAINS USING *B*-SPLINE INTERPOLATION

Alberto P. Sibileau\* and Jose J. Muñoz\*

\*Department of Applied Mathematics III, LaCàN  
Universitat Politècnica de Catalunya (UPC)  
Jordi Girona 1-3, 08034 Barcelona, Spain  
web page: <http://www-lacan.upc.es> e-mails: [j.munoz@upc.edu](mailto:j.munoz@upc.edu),  
[asibileau@gmail.com](mailto:asibileau@gmail.com)

**Keywords:** Time integration, sliding contact, energy-momentum conserving, geometrically exact beams

**Abstract.** *The design of energy-momentum algorithms for geometrically exact beams has been achieved more than 15 years ago. However, many of the desired conserving properties do not carry over into constrained systems such as beams subjected to sliding contact conditions. We here model such situation and derive a sliding contact conditions that conserves energy and momenta. Basic ingredients of the resulting formulation is the interpolation of incremental tangent-scaled rotations and a relaxation of the exact sliding condition. We also combine this formulation with a B-Spline interpolation of the beam centroid axis. In this manner, we achieve to smooth the contact loads throughout the analysis and consequently increase the stability of the numerical model. We demonstrate these advantages and the conserving properties of the algorithm with a set of two-dimensional numerical examples.*

## 1 INTRODUCTION

In the discrete approximation of nonlinear dynamics problems, even implicit time integration schemes have not been proved to ensure stability of the numerical analysis Ref. [7]. Energy- and momentum conserving algorithms aim to partially guarantee the stability of such systems (see for instance Ref. [6, 7]). In the presence of contact constraints, these properties are highly welcome due to the additional non-linearities involved [5]. Furthermore, it has been numerically verified that the spatial discretization may have detrimental effects in the dynamic response of the system [1].

We here propose a smooth interpolation with cubic  $B$ -Splines and a mid-time contact definition that ensures the energy conservation. The constraints are implemented resorting to the null-space approach and for planar geometrically exact beams.

## 2 VARIATIONAL AND ENERGY-MOMENTUM CONSERVING FORMULATIONS

### 2.1 Beam kinematics and strain definition

We here resort to the planar version of the geometrically exact beam theory (Ref. [3]). The 2D beam finite motion is presented in Fig. 1, where a vector  $\mathbf{r}$  of generalised coordinates is defined as follows:

$$\mathbf{x} = \begin{Bmatrix} \mathbf{x} \\ \theta \end{Bmatrix} = \begin{Bmatrix} X_1 \\ 0 \\ 0 \end{Bmatrix} + \begin{Bmatrix} u_1 \\ u_2 \\ \theta \end{Bmatrix} \quad (1)$$

Associated to the position vector  $\mathbf{x}$  we defined a moving frame  $\mathbf{t}_i$  attached to the beam cross-section and rotates with respect to the reference configuration  $\mathbf{e}_i$ <sup>1</sup>. The first two components of Eq. (1) give the position of the moving frame's origin, which is always located at the line of centroids. The third component of Eq. (1) denotes the angle related to the moving frame's orientation, governed by:

$$\mathbf{t}_i = \Lambda^T \mathbf{e}_i; \quad \text{with } \Lambda = \begin{bmatrix} \cos \theta & -\sin \theta & 0 \\ \sin \theta & \cos \theta & 0 \\ 0 & 0 & 1 \end{bmatrix} \quad (2)$$

From the kinematic assumptions, the 2D beam strain energy follows as,

$$\Psi = \frac{1}{2} \int_L \mathbf{N} \cdot \boldsymbol{\Gamma} dX \quad (3)$$

where  $\mathbf{N}$  are forces acting at a cross-section of the beam, and the corresponding conjugate strains  $\boldsymbol{\Gamma}$  are obtained from:

$$\boldsymbol{\Gamma} = \Lambda^T \frac{d\mathbf{r}}{dX} - \mathbf{e}_1 \quad (4)$$

Assuming for simplicity that strains are small, then the constitution may be expressed by a linear elastic relation  $\mathbf{N} = \mathbf{C} \boldsymbol{\Gamma}$ . The virtual elastic work of the beam may be then deduced as,

$$\delta\Psi = \int_L \delta\boldsymbol{\Gamma}^T \mathbf{N} dX = \int_L \delta\boldsymbol{\Gamma}^T \Lambda^T \mathbf{n} dX \quad (5)$$

where  $\delta\boldsymbol{\Gamma}$  corresponds to beam virtual strains:

$$\delta\boldsymbol{\Gamma} = \delta \left( \Lambda^T \frac{d\mathbf{r}}{dX} \right) = \Lambda^T \left\{ -[\delta\boldsymbol{\Theta}]_{\times} \mathbf{r}_{,X} + \delta\mathbf{r}_{,X_1} \right\} \quad (6)$$

<sup>1</sup>Let remark  $X_i$  are components in the reference configuration, and is assumed from now on that:  $X \equiv X_1$

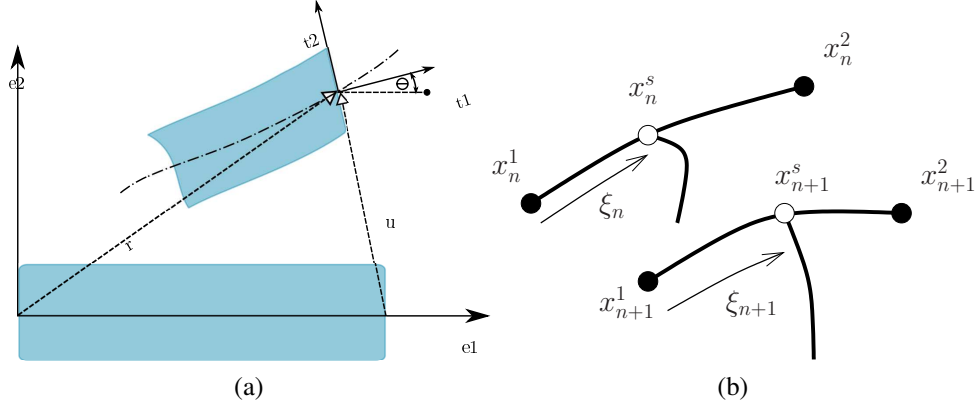


Figure 1: Finite motion of planar beam (a) and kinematics of a sliding contact condition (b)

## 2.2 Variational beam formulation.

Given the internal spatial load and moment  $\mathbf{n}$  and  $\mathbf{m}$ , and the linear and angular momentum vector  $\mathbf{L}$  and  $\mathbf{J}$ , the beam equilibrium equations,

$$\mathbf{n}' + \mathbf{n}_{ext} = \dot{\mathbf{L}} \quad (7)$$

$$\mathbf{M}' + \mathbf{M}_{ext} + \mathbf{r}' \times \mathbf{n} = \dot{\mathbf{J}} \quad (8)$$

are solved in the usual manner: premultiplying by a vector of virtual kinematics  $\delta \mathbf{r}$  and integrating by parts the resulting elastic component. After resorting to the following finite element approximation for the displacements and rotations,

$$\begin{Bmatrix} u_1 \\ u_2 \\ \theta \end{Bmatrix} = N_\alpha(X) \begin{Bmatrix} u_{1\alpha} \\ u_{2\alpha} \\ \theta_\alpha \end{Bmatrix} \quad (9)$$

and a Newmark-like time-integration algorithm, the system of equations are obtained by assembling the elemental residuals  $\mathbf{g}^e$  (see for instance Ref. [1]):

$$\mathbf{A}_e \mathbf{g}^e = \mathbf{0}$$

In the absence of external loads, the elemental residual associated to node  $\alpha$  is given by,

$$\mathbf{g}_\alpha^e = \int_{L^e} \mathbf{B}_\alpha^T \mathbf{N} dX_1 - \mathbf{f}_\alpha + \int_{L^e} \rho \begin{bmatrix} \mathbf{A} \mathbf{I} & \mathbf{0} \\ \mathbf{0} & I_r \end{bmatrix} \ddot{\mathbf{r}} dX_1$$

where  $I_r$  is tensor of inertia and the strain-displacement matrix  $\mathbf{B}_\alpha$  is given by,

$$\mathbf{B}_\alpha = \mathbf{\Lambda}^T \begin{bmatrix} N_{\alpha, X_1} & 0 & N_\alpha u_{2, X_1} \\ 0 & N_{\alpha, X_1} & -N_\alpha (1 + u_{1, X_1}) \\ 0 & 0 & N_{\alpha, X_1} \end{bmatrix}$$

## 2.3 Energy-momentum beam formulation

Alternatively, a set of residuals may be constructed by expressing the elemental total energy, sum of the kinetic ( $K^e$ ) and elastic ( $E^e$ ) energy, as follows (Ref. [7]):

$$\Delta K^e + \Delta E^e = \mathbf{R}^e \cdot \mathbf{v}_{n+\frac{1}{2}}^e$$

with  $\mathbf{v}_{n+\frac{1}{2}}^e = \frac{\mathbf{r}_{n+1}^e - \mathbf{r}_n^e}{\Delta t}$  an algorithmic mid-time velocity, and  $\mathbf{r}^e$  the set of nodal positions  $\mathbf{x}^e$  and rotations  $\theta^e$ . In this manner, by assembling the elemental residual  $\mathbf{R}^e$ , we obtain an energy-momentum conserving algorithm,

$$\mathbf{A} \mathbf{R}^e = \mathbf{0} \quad (10)$$

We note that the conservation of angular momentum and energy (in 2D and 3D problems) requires the interpolation of incremental tangent-scaled rotations:

$$\Delta\omega = N_\alpha(X)\Delta\omega^i$$

with  $\Delta\omega^i = 2 \tan(\Delta\theta^i/2)$ .

## 2.4 Incremental sliding contact conditions

The sliding condition will be implemented resorting to the master-slave approach. The position of the slave node  $\mathbf{x}^s$  is parametrized through a variable  $\xi$ . Furthermore, in order to achieve an energy conserving algorithm, the exact sliding condition  $\mathbf{x}_n^s = \sum B^i(\xi_n)\mathbf{x}_n^i$  is relaxed and replaced by the following mid-time contact condition (see Figure 1b),

$$\mathbf{x}_{n+1}^s = \sum \frac{1}{2} (B^i(\xi_n) + B^i(\xi_{n+1})) (\mathbf{x}_n^i + \mathbf{x}_{n+1}^i) - \mathbf{r}_n^s. \quad (11)$$

From this relation, and by using the notation  $B_{n+\frac{1}{2}}^i = \frac{1}{2}(B^i(\xi_{n+1}) + B^i(\xi_n))$ , the following expression for the incremental and mid-time positions may be derived:

$$\Delta\mathbf{x}^s = \sum B_{n+\frac{1}{2}}^i \Delta\mathbf{r}^i + 2 \left( B_{n+\frac{1}{2}}^i \mathbf{x}_n^i - \mathbf{x}_n^s \right) \frac{\Delta\xi}{\Delta\xi} \quad (12)$$

$$\mathbf{x}_{n+\frac{1}{2}}^s = B_{n+\frac{1}{2}}^i \mathbf{x}_{n+\frac{1}{2}}^i \quad (13)$$

which allows us to express the total energy as,

$$\Delta E = \mathbf{R}^m \cdot \mathbf{v}_{n+\frac{1}{2}}^m + \mathbf{R}^s \cdot \mathbf{v}_{n+\frac{1}{2}}^s = (\mathbf{R}^i + \mathbf{R}^s B^i(\xi_{n+\frac{1}{2}})) \cdot \mathbf{v}_{n+\frac{1}{2}}^i + \frac{2\Delta\xi}{\Delta\xi} \left( B_{n+\frac{1}{2}}^i \mathbf{x}_n^i - \mathbf{x}_n^s \right)$$

It turns out then that by solving the following equations,

$$\begin{aligned} \mathbf{R}^i + \mathbf{R}^s B_{n+\frac{1}{2}}^i &= \mathbf{0}, i = 1, \dots, N \\ \frac{2}{\Delta\xi} \sum_j \left( B_{n+\frac{1}{2}}^j \mathbf{x}_n^j - \mathbf{x}_n^s \right) \cdot \mathbf{R}^s &= 0 \end{aligned} \quad (14)$$

the total energy is conserved. The expressions on the lhs of (14) replaces the residuals in (10). It can be also deduced from condition (13) that the total angular momentum is conserved.

If instead of the contact condition in (11) we would use the exact sliding condition  $\mathbf{x}_n^s = B^i(\xi_n)\mathbf{x}_n^i$ , the relation between the mid-time positions is given by,

$$\Delta\mathbf{x}^s = B_{n+\frac{1}{2}}^i \Delta\mathbf{x}^i + \Delta\xi \frac{\Delta B^i}{\Delta\xi} \mathbf{x}_{n+\frac{1}{2}}^i \quad (15)$$

$$\mathbf{x}_{n+\frac{1}{2}}^s = B_{n+\frac{1}{2}}^i \mathbf{x}_{n+\frac{1}{2}}^i + \frac{\Delta\xi \Delta B^i}{4} \mathbf{x}_{n+\frac{1}{2}}^i \quad (16)$$

The last equation differs from (13), and therefore the conservation of angular momentum would be spoiled if the exact contact conditions, instead of equation (11) would be used.

For the situation when  $\Delta\xi \rightarrow 0$ , and in view of equation (16), we have that the exact contact condition conserves the angular momentum, and furthermore,  $\Delta B^i / \Delta\xi \rightarrow B_{n+1}^{i'}$ . Therefore, by using the incremental relation in (15), we can obtain an energy and angular momentum conserving algorithm by solving the following equations:

$$\begin{aligned} \mathbf{R}^i + \mathbf{R}^s B_{n+\frac{1}{2}}^i &= \mathbf{0}, i = 1, \dots, N \\ \sum_j B_{n+1}^{j'} \mathbf{x}_{n+\frac{1}{2}}^j \cdot \mathbf{R}^s &= 0 \end{aligned} \quad (17)$$

Note that in fact only equation (17)<sub>2</sub> has been modified, while equations (17)<sub>1</sub> remain unchanged.

### 3 CUBIC B-SPLINE INTERPOLATION

The weak form of the equilibrium equations are now solved by discretizing the kinematic variables  $\mathbf{r}$  and  $\theta$  with a set of  $n_e$  cubic *B-Splines*, which result in a curve  $\mathbf{C}(\xi) = B_{i,p}(\xi)\mathbf{P}_i$ . The curve is shaped according to  $n + 1$  *control points*  $\mathbf{P}_i$  and the corresponding basis function  $B_{i,p}(\xi)$ , defined over a parametric space  $0 \leq \xi \leq 1$  and by the chosen order  $p = 3$ . For further details, see Ref. [8].

The support of each basis function is determined from a *knot vector*  $\mathbf{k}$  of the form,

$$\mathbf{k}^T = \left\{ \underbrace{0, \dots, 0}_{p+1}, \xi_1, \dots, \xi_{m-2p-1}, \underbrace{1, \dots, 1}_{p+1} \right\}_{m+1},$$

which has  $m + 1$  *knot values* and  $m = n + p + 1$ . The *knot spans*  $[\xi_i, \xi_{i+1})$  are used to define the basis functions, that are constructed following a recursive formulae for **all** knot values in  $\mathbf{k}$ :

$$\begin{aligned} B_{i,0}(\xi) &= \begin{cases} 1 & \text{if } \xi_i \leq \xi < \xi_{i+1} \\ 0 & \text{otherwise} \end{cases} \\ B_{i,p}(\xi) &= \frac{\xi - \xi_i}{\xi_{i+p} - \xi_i} B_{i,p-1}(\xi) + \frac{\xi_{i+p+1} - \xi}{\xi_{i+p+1} - \xi_{i+1}} B_{i+1,p-1}(\xi) \end{aligned} \quad (18)$$

Following the previous, the set of cubic *B-Splines* can be used as a standard FE interpolation. Therefore, the set of shape functions in Eq. (9) is the replaced by the basis *Bernstein polynomials*  $B_{i,3}(\xi)$  and the associated set of nodes corresponds to the control points  $\mathbf{P}_i$ . It still remains to describe how  $\mathbf{P}_i$  and  $\mathbf{k}$  are obtained for the initial beam geometry. A local cubic interpolation is performed through a set of  $n_e$  elements, whose *start* and *end* coordinates are previously determined in the initial beam geometry. The methodology resorts to the algorithm described in Ref. [2]. Let only remark that the resultant number of nodes for the cubic *B-Spline* interpolation has the following relation  $n = 2n_e + 1$ .

However, it is worth to note two important differences when dealing with *B-Splines* rather than FE interpolation of beams. First, the connectivity must be changed according to the specific local support of the basis functions  $B_{i,p}(\xi)$ . Moreover, note the *B-Spline* elements are defined for  $\xi \in [0, 1]$ , which corresponds for the the *whole* entire beam geometry. Thus, the position of the Gauss points in each element varies and additional storage is needed for the elemental shape functions values.

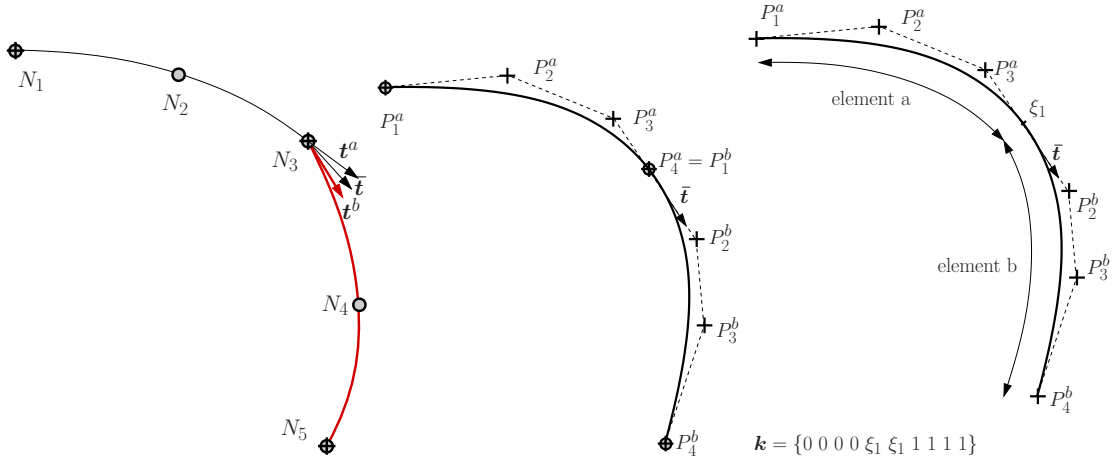


Figure 2: Definition of B-Spline from initial nodes of the beam.

## 4 RESULTS

### 4.1 The flying spaghetti

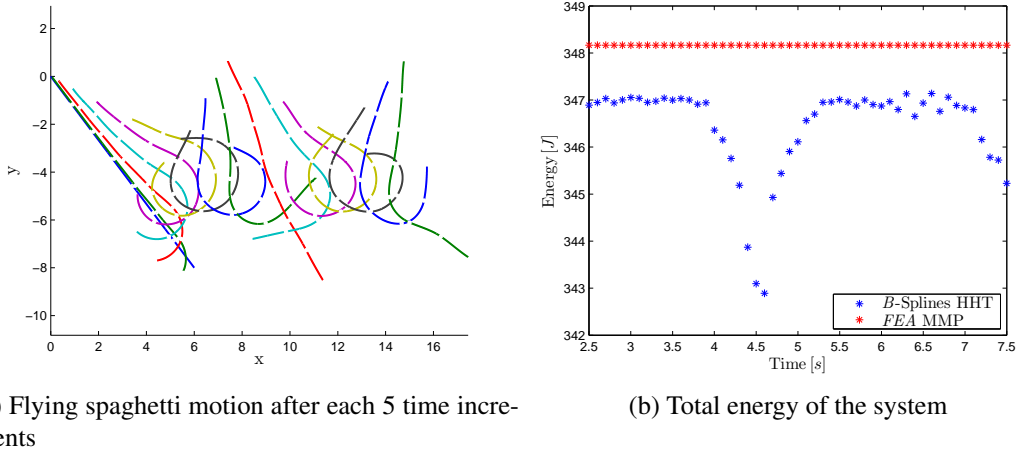
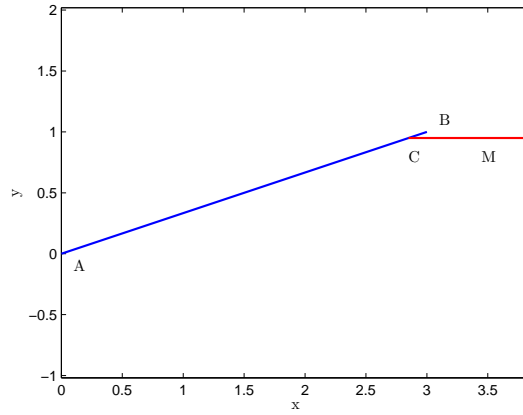


Figure 3: Numerical simulation of nonlinear dynamics

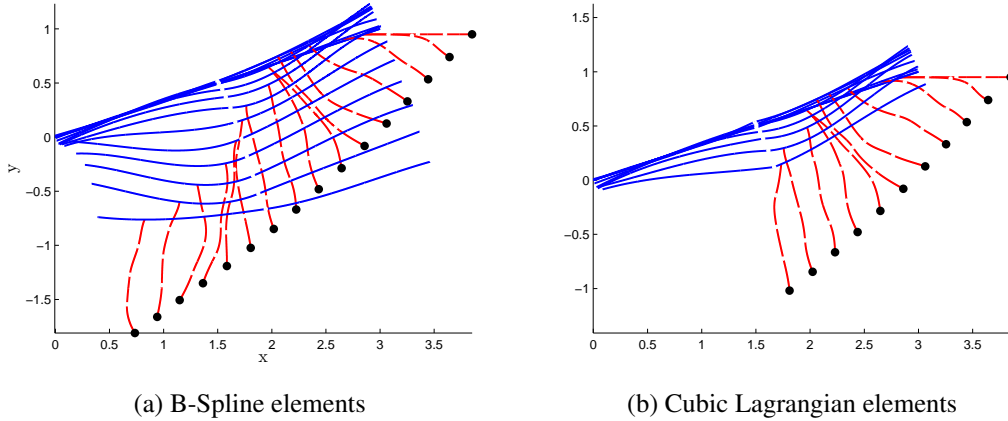
A flexible rod with free ends, initially placed in an inclined position, is subjected to a torque and force applied simultaneously at one end (Ref. [4]). External forces and moment are removed at the same time  $t = 2.5$ , and the free flight simulation is performed subsequently till  $t = 7.5$ . The sequence of motion is presented in Figure 3a, where the beam is discretized with 7 cubic *B*-Splines segments (see knots depicted) and integrated in time using the trapezoidal rule and  $\Delta t = 0.1$ .

The same example has been also modeled using the energy conserving modified mid-point rule (MMP) described in Ref. [7], and with 10 linear finite elements. The evolution of the total energy of the system in free flight is shown in Figure 3b, which as expected remains constant only for the EC scheme. However, we point out that when using more than 3 cubic finite elements the analysis failed to converge, while no convergence problems were encountered even for 15 cubic BSpline elements.



(a)

Figure 4: Free sliding mass example



(a) B-Spline elements

(b) Cubic Lagrangian elements

Figure 5: Motion simulation for the free sliding mass. Plot after each 2 time increments.

## 4.2 The free sliding mass

This example involves two flexible beams connected with a sliding joint. The initial configuration is depicted in Fig. 4 and the material and geometrical properties are identical for both beams, except their lengths:

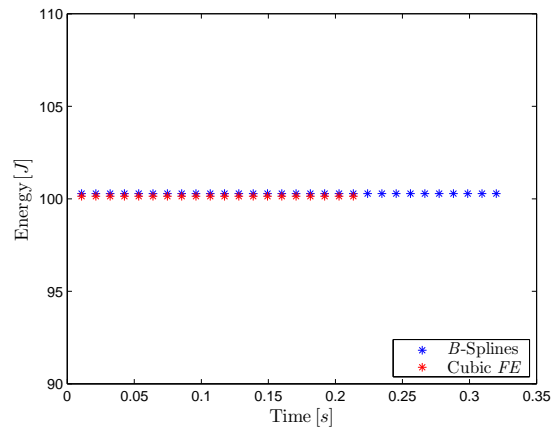
$$A = \{0 \ 0\}; \quad B = \{3 \ 1\}; \quad M = \{C(1) + 1 \ C(2)\}$$

$$EI = 20; \quad \rho I = 1.6e^{-2}; \quad AE = 100; \quad \rho A = 8e^{-2} \quad \text{and} \quad \nu = 0.3$$

A mass of 1 kg is attached as depicted, at point M. Note that point M is defined with respect to point C, which is in fact positioned at a defined tolerance from beam tip B (in the present case tolerance is  $1/20$  of beam AB length). Finally, the mass is subjected to an initial velocity  $v_0 = \{-10 \ -10\}$ .

In the following situations, beam AB and BM are discretized using two and four elements respectively, and time integration is performed with a constant time-step  $\Delta t = 0.01067$ . A comparison is done between the performance of B-Spline against cubic Lagrangian interpolation. As it is shown in Fig. 5, the solution convergence fails at the contact transition when the cubic interpolation is used.

The conservation of energy is shown also for the present example in Fig. 6



(a)

Figure 6: Energy conserving properties

## REFERENCES

- [1] J. Muñoz and G. Jelenic. Sliding joints in 3D beams: Conserving algorithms using the master-slave approach. *Multibody Syst. Dyn.*, **16**,237-261, 2006.
- [2] J. Muñoz. Modeling unilateral frictionless contact using the null-space method and cubic B-Spline interpolation. *Comput. Methods Appl. Mech. Engng.*, **197**,979-993, 2008.
- [3] J.C. Simo and L. Vu-Quoc. A three-dimensional finite-strain rod model. Part II: computational aspects. *Comp. Meth. Appl. Mech. Engng.*, **58**,79-116, 1986.
- [4] J.C. Simo and L. Vu-Quoc. On the Dynamics of Flexible Beams Under Large Overall Motions - The Plane Case: Part II. *ASME J. of Appl. Mech.*, **53**,849-854, 1986.
- [5] C. Hesch and P. Betsch. A mortar method for energy-momentum conserving schemes in frictionless dynamic contact problems. *Int. J. Numer. Meth. Engng.*, **77**,1468-1500, 2009.
- [6] O.A. Bauchau and C.L. Bottasso. On the Design of Energy Preserving and Decaying Schemes for Flexible, Nonlinear Multi-Body Systems. *Comput. Methods Appl. Mech. Engng.*, **169**,61-79, 1999.
- [7] N. Stander and E. Stein. An energy-conserving planar finite beam element for dynamics of flexible mechanisms. *Engng. Comput.*, **16**,60-85, 1996.
- [8] L. Piegl and W. Tiller. *The Nurbs Book*. Second edition, Springer, Germany 1997.
- [9] I. Temizer and P. Wriggers and T.J.R. Hughes Contact treatment in isogeometric analysis with NURBS *Comput. Methods Appl. Mech. Engng.*, **200**,1100-1112, 2011.